NDA based feedforward sampling frequency synchronization for OFDM systems

Erik Oswald
Department of Transmission Systems
Fraunhofer Institute for Communication Systems
Munich, Germany
erik.oswald@esk.fraunhofer.de

***Abstract*—In addition to the performance advantages of new transmission techniques, implementation aspects are of increasing interest. Accordingly, modern receiver architectures use non-synchronized sampling. Timing adjustment is completely performed in the digital domain. In this contribution we will present a new digital approach for sampling frequency synchronization based on non-synchronized sampling in OFDM systems. Compared to known feedback techniques, an advantageous method based on NDA feedforward processing is applied. Because this is a novel technique, particular emphasis is placed on timing error detection. This calculates the sampling frequency offset directly from the incoming time domain samples. Based on this information, a control parameter for the correction by interpolation can be derived. The solution presented offers many advantages and meets the requirements of modern receiver technology. It can be used for WLAN systems based on OFDM modulation.**

Keywords-OFDM; sampling frequency synchronization; timing error detection; feedforward processing

I. INTRODUCTION

Flexibility based on mobility is of fundamental importance in today's fast moving information age. Wireless communication contributes significantly to this development. Over the past several years Orthogonal Frequency Division Multiplexing (OFDM) has been applied successfully to wireless applications (e.g. [1]). In addition to the performance advantages of new transmission techniques, implementation aspects are of increasing interest. Today there is a strong demand for completely digital transmitter and receiver systems. As opposed to analog hardware, digital receiver functions offer many favorable features in terms of flexibility and integratability. In the course of this trend, many excellent digital receiver implementations have been proposed (e.g. [2]). It is a known problem that OFDM is highly sensitive to incorrect synchronization. Digital techniques for the correction of OFDM symbol timing and frequency offsets have been an important subject of investigations [3]-[5]. But there is a third part of synchronization. Only a limited number of proposals are available to describe digital sampling frequency synchronization for OFDM (e.g. [6]). To avoid Inter-Carrier Interferences (ICI), the correction of occurring sampling frequency deviations is a mandatory requirement [7]. Furthermore, sampling constitutes the interface between analog and digital signal processing and thus influences the receiver design significantly. The process of sampling frequency synchronization based on an optimized digital implementation will be addressed in this paper. So-called non-synchronized sampling fulfills the demands of an all-digital receiver design. This is realized by a fixed free-running sampling clock. During normal operations, an offset between transmitter and receiver sampling frequency will occur, causing a phase rotation and ICI [7]. To prevent significant performance degradation, efficient post-processing must be performed. This is divided into the main tasks of timing error detection (TED) and timing error correction (TEC). Sampling frequency synchronization based on TED and TEC can be achieved using a feedback loop. Several techniques using data-aided (DA) (e.g. decision-directed) TED have been the subjects of investigations. For OFDM the principle depicted in of Fig. 1 is normally used. The nominal sample period T_S is affected by the deviation ΔT_S.

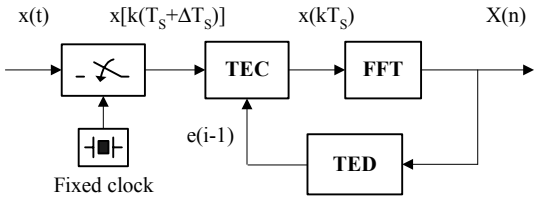

Figure 1. Feedback synchronization

The drawbacks of this synchronization result from the used phase-locked loop (PLL). This requires large amounts of board space, power consumption and circuit complexity. The technique which will be presented here offers a new advanced approach for digital sample synchronization. Instead of feedback processing, an efficient non-data-aided (NDA) feedforward technique is applied. Fig. 2 shows the general structure of the feedforward synchronization.

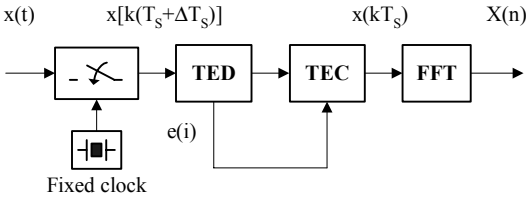

Figure 2. Feedforward synchronization

Compared to known feedback techniques, it has many advantageous features. Its major advantage is that it provides rapid synchronization and guaranteed stability, which is important especially in mobile communication systems. The low design complexity allows for a modern single-chip design and lower implementation costs.

II. OFDM TRANSMISSION

OFDM is a well-known transmission technique and has been described in many publications (e.g. [2]). Therefore, only a brief description of this technique will be given here. At the transmitter the serial input data are divided into groups of ld(M) bits and converted in complex symbols $a_i(n)$ resulting from an M-ary alphabet of N constellation points. These complex symbols are modulated on N sub-carriers using the inverse discrete Fourier transform (IDFT). To prevent Inter-Symbol Interferences (ISI), after parallel-to-serial conversion each OFDM symbol is preceded by a copy of the last N_G samples (guard interval). This extension results in a total symbol duration of $T_{OFDM}=(N+N_G)/f_S$, comprising $N+N_G$ samples. After digital-to-analog conversation, the signal is transposed into the RF range. Before the transmission over the channel, the spectrum has to be limited by an analog band-pass filter. Depending on the RF channel characteristics, the received OFDM signal is influenced by the multi-path propagation. According to the maximal channel delay τ_{max}, the OFDM symbol is enlarged and thus disturbed by unwanted symbol overlays. For a channel impulse response (CIR) not longer than the guard interval ($\tau_{max} \le T_G$), disturbing ISI can be avoided. After passing the transmission channel, the signal is processed by the receiver front-end. Subsequent demodulation at the receiver is performed by the inverse transmitter operations. Equation (1) describes the received samples of an OFDM symbol with index i by its complex baseband representation.

$$y_i(k) = \sum_{n=0}^{N-1} \tilde{a}_i(n) \cdot e^{j2\pi \frac{kn}{N}} \qquad (1)$$

In (1), the variable $\tilde{a}_i(n)$ describes the product of $a_i(n)$ and the channel transfer function H(n). A constant channel characteristic at least for one OFDM symbol was assumed. For the description of the effects of imperfect sampling, the transformation of (1) into the frequency domain by the discrete Fourier transform (DFT) must be performed. By using some mathematical operations the resulting expression can be divided into the absolute and the phase part (2) [7].

$$Y_i(n') = \frac{\tilde{a}_i(n')}{N} \cdot \sum_{n=0}^{N-1} \frac{\sin\left[\pi\left(\frac{n}{1-\Delta_f} - n'\right)\right]}{\sin\left[\frac{\pi}{N}\left(\frac{n}{1-\Delta_f} - n'\right)\right]} \cdot e^{j\frac{N-1}{N}\pi\left(\frac{n}{1-\Delta_f} - n'\right)} \qquad (2)$$

Equation (2) describes the resulting spectrum for $0 \le n' \le N-1$. Thereby a relative sampling frequency deviation $\Delta_f=(f_{trans}-f_{rec})/f_{trans}$ was considered. To show the influence of the sub-carriers on the received spectrum, a distinction between n and n' was introduced. The index n' describes the resulting spectral components after the DFT. By the index n the influence of the neighbored sub-carriers for each index n' can be shown. The last term of (2) shows that a phase rotation will occur. The changes in phase depend linearly on the carrier index and lead to a rotation of the complex constellation points around the center of the signal space diagram. Using a simple frequency domain equalizer consisting of one complex tap for each sub-carrier allows the correction of this phase modification. More critical are ICI, which increase with the sub-carrier index and destroy the signal orthogonality. ICI result from the processing of a non-ideal sampled OFDM symbol by the DFT. The resulting spectral components are located between the maxima and the equidistant zero points of an orthogonal spectrum. Because of this effect, each spectral component is influenced by spectral components of every other transmitted sub-carrier. This effect can be calculated using the absolute value of (2). A further classification of $|Y_i(n')|$ is achieved by the separation of useful (n'=n) and disturbing (n'≠n) spectral components. The result of $|Y_i(n')|_{n'\neq n}$ describes the summation of all interfering spectral components for the index n'. By $|Y_i(n')|_{n'=n}$ only the useful spectral component for the index n' will be considered. Several investigations have shown that efficient sampling frequency synchronization is a mandatory requirement to prevent a significant SNR degradation by the loss of sub-carrier orthogonality [7].

III. SAMPLING FREQUENCY OFFSET DETECTION

A. Principle

Digital sampling frequency synchronization comprises two main tasks. TEC is normally performed by interpolation. Because interpolation filters have been studied thoroughly in the past, TEC by interpolation is not described in detail in this paper (e.g. [8]). For interpolation control the sampling frequency deviation must be detected (TEC). Based on this information, a control parameter can be derived. In the following, we propose a new approach for the detection of the sampling frequency deviation allowing feedforward synchronization. As described above, each OFDM symbol is preceded by a copy of the last N_G samples. Therefore, for an ideal sampling frequency ($\Delta f_S=0$) at the receiver two similar sample sequences per OFDM symbol can be observed. For simplification these samples sequences will be named Seq-1 and Seq-2 (Fig. 3).

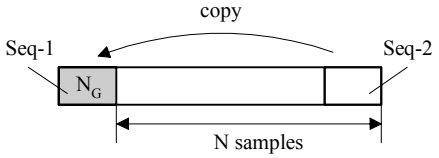

Figure 3. OFDM symbol including Seq-1 and Seq-2

From oscillator properties we can derive that the sampling frequency deviation Δf_S will only be changing slowly [9].

Therefore, at least for one OFDM symbol a constant sampling frequency deviation Δf_S can be assumed. This property causes the sample sequences Seq-1 and Seq-2 to differ fractionally. Because corresponding sample pairs of Seq-1 and Seq-2 are located N samples apart, the amplitudes differ by the effect of $N\Delta T_S$. These differences can be compared with the effect of a parameter-controlled interpolation (Fig. 4) and can be used for the calculation of ΔT_S.

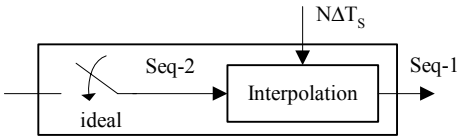

Figure 4. Model of imperfect sampling

Fig. 4 shows a simplified model of imperfect sampling for an OFDM symbol comprising $N+N_G$ samples. It illustrates the sample sequences Seq-1 (guard interval) and the repetition in Seq-2. The primary objective of the new sampling frequency detection is to calculate the interpolation parameter $N\Delta T_S$. For this purpose a mathematical description of Seq-1 and Seq-2 according to Fig. 4 must be found. Considering efficiency and numerical effort, a solution can be achieved by using the polynomial-based interpolation formula of Lagrange (3) [8].

$$\underline{y} = y_1 \cdot \frac{(\underline{x}-x_2)(\underline{x}-x_3)\ldots(\underline{x}-x_m)}{(x_1-x_2)(x_1-x_3)\ldots(x_1-x_m)} + \cdots + y_m \cdot \frac{(\underline{x}-x_1)(\underline{x}-x_2)\ldots(\underline{x}-x_{m-1})}{(x_m-x_1)(x_m-x_2)\ldots(x_m-x_{m-1})} \tag{3}$$

In the unique polynomial of degree m-1 the samples of Seq-1 are described by $x_{1\ldots m}$ and $y_{1\ldots m}$. Based on these samples and $\underline{x}$, the amplitude $\underline{y}$ of Seq-2 can be calculated. In expression (3) the variable $\underline{x}$ contains the information of $N\Delta T_S$, which describes the difference in time between Seq-1 and Seq-2. To illustrate the relations of (3), Fig. 5 shows Seq-1 and Seq-2 for a cubic polynomial (m=4).

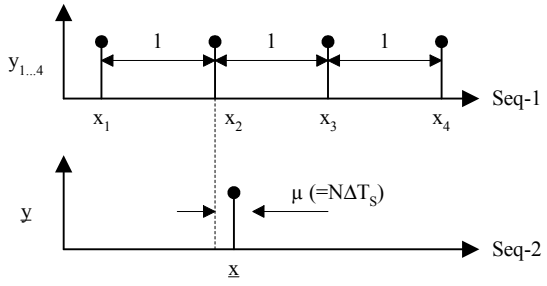

Figure 5. Relations of Seq-1 and Seq-2

Because the amplitudes of Seq-1 and Seq-2 differ only by the effect of $N\Delta T_S$ (=μ), an ideal sample period (T_S=1) for Seq-1 can be assumed. Based on this assumption, the differences of the numerator of equation (3) can be expressed in a simplified manner (4).

$$\begin{aligned} \underline{x}-x_1 &= \mu+1 & \underline{x}-x_2 &= \mu \\ \underline{x}-x_3 &= \mu-1 & \underline{x}-x_4 &= \mu-2 \end{aligned} \tag{4}$$

Using these expressions and some mathematical operations leads to a simplified form of the polynomial (3). All differences of the numerator and the denominator have been replaced by integers and the parameter μ (5).

$$\begin{aligned} \underline{y} = & \left(-\frac{1}{6}\cdot y_1 + \frac{1}{2}\cdot y_2 - \frac{1}{2}\cdot y_3 + \frac{1}{6}y_4\right)\cdot\mu^3 \\ & + \left(\frac{1}{2}\cdot y_1 - y_2 + \frac{1}{2}\cdot y_3\right)\cdot\mu^2 \\ & + \left(-\frac{1}{3}\cdot y_1 - \frac{1}{2}\cdot y_2 + y_3 - \frac{1}{6}y_4\right)\cdot\mu \\ & + y_2 \end{aligned} \tag{5}$$

Expression (5) represents an equation for cubic interpolation and includes the samples of Seq-1 and Seq-2. The parameter μ contains the required information about $N\Delta T_S$. Because $\underline{y}$ and $y_{1\ldots m}$ are known at the receiver and $\mu_{1\ldots m-1}$ can be derived by root extraction, it must be possible to separate ΔT_S. After transposing (5), the values $\mu_{1\ldots m-1}$ can be calculated by a computationally efficient eigenvalue method [10]. Because the correct value of $\mu_{1\ldots m-1}$, which describes the true amount of $N\Delta T_S$, must be real, we have implemented a simple algorithm for searching the lowest imaginary part of $\mu_{1\ldots m-1}$. To receive ΔT_S, finally, μ must be normalized by the number of samples located between Seq-1 and Seq-2. For a typical OFDM scenario this number is N. The principle of the described timing error calculation is illustrated by Fig. 6.

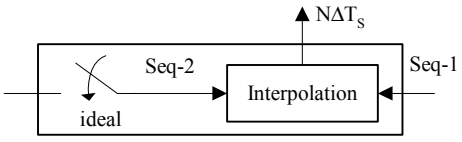

Figure 6. Operating principle of the TED

B. Channel influence

Of course, for real transmission scenarios different channel influences must be considered. An essential property is the multipath propagation. The resulting channel delay τ leads to larger symbol duration. Depending on τ_{max} each sample at the receiver is influenced by adjacent samples. In this way, the sample sequences Seq-1 and Seq-2 differ by a second effect, which disturbs the results of the TED described. Therefore, for the calculation of the sampling frequency deviation Δf_S by the technique presented, an essential requirement must be fulfilled. Both sample sequences must include samples which differ only by the effect of the sampling frequency deviation Δf_S. These samples are influenced by the channel and adjacent samples in the same manner. It is obvious that not all samples of Seq-1 and Seq-2 fulfill this requirement. Only a short range of N_{ave} samples within Seq-1 and Seq-2 can be used for the calculation of the sampling frequency deviation Δf_S. In the following the

CIR was assumed constant at least for one OFDM symbol period T_{OFDM}. Based on this condition, the convolution of the CIR and the OFDM symbol corresponds to the operation of a time invariant FIR filter of length N_{tap}. The filter taps result from the coefficients of the discrete CIR and describe N_{tap} propagation paths with the delay $\tau_0 \ldots \tau_{N_{tap}-1}$. Fig. 7 illustrates the channel influence resulting from the convolution of the CIR and the OFDM symbol.

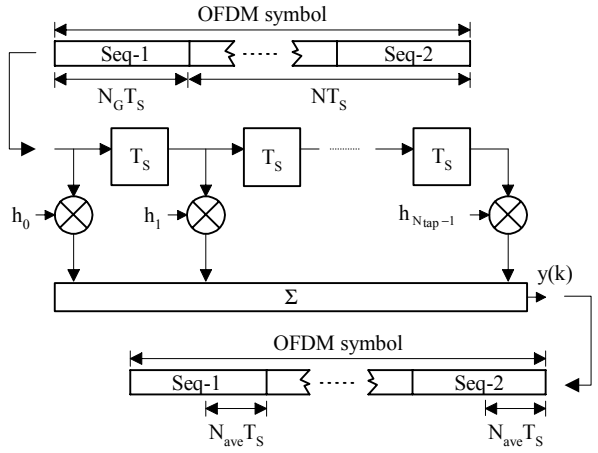

Figure 7. Channel influence

Because of channel memory, after the FIR filter all samples of Seq-1 and Seq-2 are influenced by adjacent samples. Therefore, assuming an ideal sampling frequency ($\Delta f_S=0$), after filtering only a short range of N_{ave} samples within Seq-1 and Seq-2 will be nearly identical. For the calculation of these samples the filter registers include only samples of Seq-1 or Seq-2. At this point the CIR lies inside the boundaries of Seq-1 and Seq-2. Of course, the condition $N_G>N_{tap}$ is a mandatory requirement. Assuming a sampling frequency deviation ($\Delta f_S\neq0$), the amplitudes of the N_{ave} samples of Seq-1 and Seq-2 differ only by the effect of $N\Delta T_S$. These samples can be used for the calculation of the sampling frequency deviation Δf_S. Based on the properties described, it is necessary that the N_{ave} samples of Seq-1 and Seq-2 be found. Because the CIR corresponds to a nearly exponential function and the length of the guard interval is sufficiently dimensioned, there are enough samples of Seq-1 and Seq-2 which are only negligibly or not influenced by samples outside of Seq-1 and Seq-2. In spite of the channel influence, these samples differ only by the effect of $N\Delta T_S$. To find the range of the N_{ave} samples, two different methods can be used. Using knowledge about the CIR at the receiver results in a simple solution for finding the interval N_{ave} ($\approx N_G-N_{tap}$). The second method requires the calculation of ΔT_S for all N_G samples of Seq-1 and Seq-2. Subsequently, intervals including different numbers of ΔT_S are composed. The interval with the lowest standard deviation provides the desired values of ΔT_S. To find the lowest standard deviation, a simple search algorithm can be used. For a further optimization, the received interval including N_{ave} values of ΔT_S was filtered by a simple median filter. After this operation, additional noise rejection is achieved by the calculation of the mean value of ΔT_S. Moreover, the received interval N_{ave} indicates the sample index for the calculation of ΔT_S for the following OFDM symbols.

C. *Simulation results*

The functionality of the sampling frequency deviation detector described has been verified by several simulations. A typical OFDM-based WLAN scenario was applied (N=64, T_{OFDM}=4µs, T_G=0.8µs). Moreover, over-sampling by a factor of 4 was used. During simulations, the relative sampling frequency deviation Δ_f was changed after duration of 10 OFDM symbols (Δ_f: 100 ppm, -100 ppm, 200 ppm, -50 ppm, 150 ppm). The detection accuracy is most affected by the channel influence. Therefore, in addition to AWGN, different channel models corresponding to realistic inhouse scenarios were applied [11]. The first channel model corresponds to a typical office environment with a maximum delay spread of $\Delta\tau_{max}$=390ns. Using a guard interval with a duration of T_G=800ns results in uncritical offset detection. Fig 8 shows the sampling frequency deviation detected and the appropriate deviation from the ideal detection.

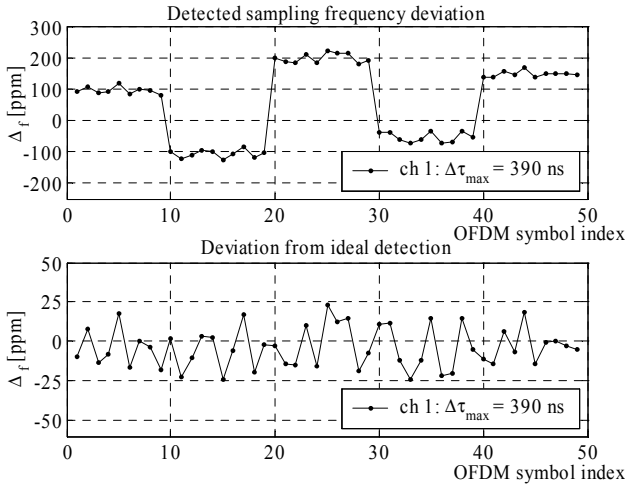

Figure 8. Detected sampling frequency deviation ($\Delta\tau_{max}$=390ns)

The upper figure shows that the detected sampling frequency deviation Δ_f is immediately available without any acquisition time after changing the induced sampling frequency deviation. The lower figure shows the deviation from the ideal detection result. Remaining deviations from the ideal detection fall below ±25 ppm. Fig. 9 shows a more critical case. The channel model used corresponds to a typical large open space environment. The maximum delay spread amounts $\Delta\tau_{max}$=730ns. Using a guard interval with a duration of T_G=800ns leads to a more critical offset detection. Because for averaging only a short range of N_{ave} values can be used, the results of Δ_f will be highly sensitive to noise. Remaining deviations exceed the relative sampling frequency deviation of ±25ppm.

The simulations have shown that AWGN will be the limiting factor. For simulations, an AWGN resulting in the SNR of 30 dB was applied. More critical noise properties

require further operations for noise rejection in addition to the median filter and averaging of ΔT_S.

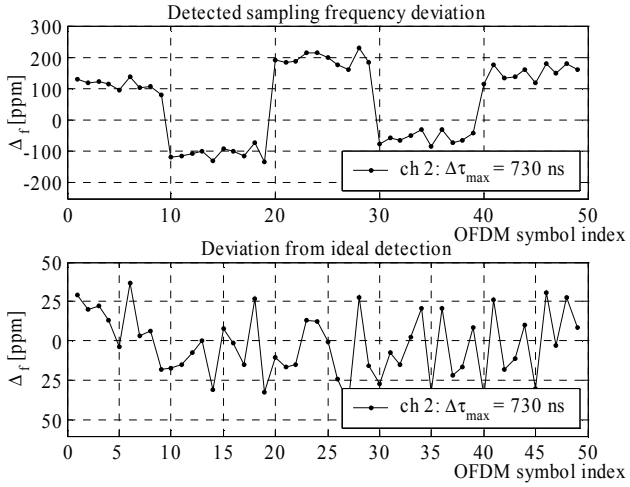

Figure 9. Detected sampling frequency deviation ($\Delta\tau_{max}$=730ns)

IV. IMPLEMENTATION ASPECTS

In this paper, particular emphasis was placed on TED. Based on the results of the described technique, timing error correction was performed by parameter-controlled interpolation. The well-known Farrow structure of a cubic interpolator was applied [8]. Fig. 10 shows the complete structure of sampling frequency synchronization.

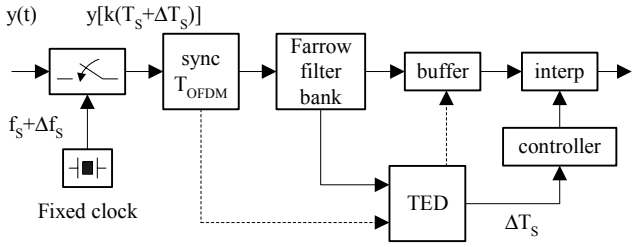

Figure 10. Sampling frequency synchronization

After sampling using a free-running sampling clock, OFDM symbol synchronization is performed [5]. This operation provides OFDM symbol timing. The remaining timing offset (ΔT_S<0,5T_S) is calculated by the described technique of TED. Finally, interpolation is performed for each OFDM symbol using an interpolation parameter derived from ΔT_S. Because interpolation is performed per OFDM symbol, the interpolation parameter consists of a vector of length N. It is important to mention that many results from the cubic interpolation technique can be used for TED. Therefore, the calculation of the Farrow filter bank was separated from the original interpolation process. In this way the numerical effort can be reduced significantly. Because of the computing time of the TED, after the Farrow filter bank the samples must be delayed by a buffer. This buffer can be controlled by the TED. With this approach, the remaining interpolation block (interp) consists only of multiplications by the interpolation parameter.

V. CONCLUSION

OFDM systems are highly sensitive to incorrect synchronization. To prevent a significant SNR degradation, efficient sampling frequency synchronization must be performed. Free-running sampling with subsequent post-processing in the digital domain fulfills the requirements of modern receiver implementations. Therefore, we have proposed in this paper an advantageous feedforward synchronization technique based on a new sampling frequency offset detector allowing free-running sampling. The new algorithm can be used for OFDM systems. It exploits a cyclic signal repetition and operates only in the time domain. Because this is the essential component of the feedforward sampling frequency synchronization, particular emphasis is placed in this paper on TED. In addition to the operation of timing error detection, the channel influence was investigated and an algorithm for excluding resulting effects was explained. Moreover, the functionality was verified by appropriate simulations. The feedforward processing is the main feature of the synchronization technique proposed here. Compared to known feedback techniques, it offers many advantages in terms of implementation and functionality. Without any acquisition time, sampling frequency synchronization providing optimal stability can be achieved. Because of the advantages and considering the necessary system requirements, the technique presented offers an interesting solution for sampling frequency synchronization in OFDM-based inhouse communication systems using free-running sampling.

REFERENCES

[1] IEEE Std 802.11a-1999, Part 11: Wireless LAN Medium Access Control (MAC) and Physical Layer (PHY) specifications: High-Speed Physical Layer in the 5 GHz Band, 1999.

[2] M. Speth, A. Fechtel, G. Fock, H. Meyr, "Optimum Receiver Design for Wireless Broad-Band Systems Using OFDM-Part 1", IEEE Trans. Commun., vol. 47, no. 11, pp. 1668-1677, Nov. 1999.

[3] F. Claßen, H. Meyr, "Synchronization Algorithms for an OFDM System for Mobile Communication", Codierung für Quelle, Kanal und Übertragung, Berlin: VDE-Verlag, vol. 130, ITG-Fachbericht, pp. 105-113, 1994.

[4] T. M. Schmidt, D. C. Cox, "Robust Frequency and Timing Synchronization for OFDM", IEEE Trans. Commun., vol. 45, pp. 1613-1621, Dec. 1997.

[5] J. van de Beek, M. Sandell, P. Börjesson, "ML Estimation of Time and Frequency Offset in OFDM Systems", IEEE Trans. Signal Processing, vol. 45, pp. 1800-1805, July 1997.

[6] T. Pollet, M. Peeters, "A New Digital Timing Correction Scheme for DMT Systems Combining Temporal and Frequential Signal Properties", in Proc. IEEE Int. Conf. on Commun., vol. 3, pp. 1805-1808, June 2000.

[7] T. Pollet, P. Spruyt, M. Moeneclaey, "The BER Performance of OFDM using Non-synchronized Sampling", Proc. of GLOBECOM, pp. 253-257, Dec. 1994.

[8] L. Erup, F. M. Gardner, R. A. Harris, "Interpolation in digital modems – Part: 2: Implementation and performance", IEEE Trans. on Commun., vol. 41, no. 6, pp. 998-1008, June 1993.

[9] C. Muschallik, "Influence of RF Oscillators on an OFDM Signal", IEEE Trans. Consumer Electronics, vol. 41, no. 4, pp. 592-603, June 1995.

[10] B. T. Smith, J.M. Boyle, J.J. Dongarra, B.S. Garbow, Y. Ikebe, et al., Matrix Eigensystem Routines – EISPACK Guide, Lecture Notes in Computer Science, vol. 6, 2nd edition, Springer-Verlag, 1976.

[11] ETSI EP BRAN, J. Medbo, P. Schramm, "Channel Models for HIPERLAN/2 in Different Indoor Scenarios", ETSI BRAN 3ERI085B, 1998.